J Polym Res (2016) 23:44
DOI 10.1007/s10965-016-0936-2

ORIGINAL PAPER

Preparation and characterization of polystyrene sulfonic acid-co-maleic acid copolymer modified silica nanoparticles

Sung-Hwa Lin [1] · Sun-Mou Lai [1] · Chih-Ming Lin [1] · Ching-Wei Chou [1] · Chih-Hung Lee [1]

Received: 4 August 2015 / Accepted: 5 February 2016

Abstract Two types of silanes, including 3-glycidoxypropyltrimethoxysilane (GPTMS) and 3-aminopropyltriethoxysilane (APTES), were grafted onto polystyrene sulfonic acid-co-maleic acid (PSSA_MA) first, followed by the grafting reaction to the silica surface. The modification of PSSA_MA onto silica was confirmed through FTIR (Fourier transform infrared spectrum), NMR (Nuclear magnetic resonance), and TGA (Thermogravimetric analysis). The grafting ratio of PSSA_MA via APTES with 1-ethyl-3-(3-dimethylaminopropyl)-carbodiimide (EDC) activation reached 18.0 %. As for GPTMS case, the grafting ratio reached 14.4 %, which was slightly lower than that of APTES case. The grafting mechanisms for both cases were elucidated. The epoxysilane was found to react with maleic acid groups on PSSA_MA only. On the other hand, the aminosilane not only interacted with sulfonic groups but also activated maleic acid groups via EDC. However, without the use of the coupling agent, the grafting degree of PSSA_MA was only 3 %, which signified the essential role of coupling agents in this organically modified silica. The average particle size of silica was around 200 nm with or without organic modification from transmission electron microscopy (TEM) and Zetasizer analysis. The APTES-modified samples showed the highest improvement in the ion adsorption capacity in all investigated cases.

Keywords Polystyrene sulfonic acid-co-maleic acid · Silica · Grafting to · Coupling agent · Aminosilane · Epoxysilane

Introduction

The significance of interfacial interaction between the organic matrix and dispersed inorganic particles through the high interfacial area was greatly recognized in attaining the best performance of nanocomposites. One of the widely used approaches to produce inorganic fillers like nanosilica is the sol–gel method which normally processes at low processing temperatures with the advantage of energy savings [1]. Silica prepared through the sol–gel process can be modified with various types of functionality to give organically modified silica for versatile applications. Philipp et al. [2] and Wilkes et al. [3] conducted pioneering works on this modification to prepare organically modified silicate, termed ORMOSIL or CERAMER, using various types of alkoxysilanes.

Polymeric adsorbents have been received much attention as an emerging alternative to activated carbon in light of their tailored surface chemistries, adjustable mechanical properties and pore sizes, as well as cost-competitive regeneration processes [4]. In order to expand the application, polymer hybrid adsorbents are expected to combine merits from both inorganic and organic materials. Pan et al. enhanced lead removal by polymer-based zirconium phosphate, in which the negatively charged sulfonic acid groups on the polymer matrix would facilitate the permeation and pre-concentrated lead ion from solution to the polymer surface [5]. Functional molecules like sulfonic acid, thios, and amino groups were quite effective in removing metal ions as well. Qu et al. [6] found that the sulfonic acid-loaded silica microsphere could effectively remove heavy metal ions (Pb^{2+}, Cd^{2+}, and Cu^{2+}) in the solution via the electrostatic interaction. Other studies on the thiol

✉ Sun-Mou Lai
smlai@niu.edu.tw

[1] Department of Chemical and Materials Engineering, National I-Lan University, I-Lan 260, Taiwan, Republic of China

Published online: 13 February 2016

groups and their conversion to sulfonic groups for the metal ions were reported as well by exploiting bi-functionalized silica [7]. Wang et al. [8] prepared (2-acrylamido-2-methylpropanesulfonic acid)/silica (AMPS-silica) hybrid adsorbents, on which multifunctional groups including carboxyl, amino, and sulfonic acid were loaded. The prepared hybrids were investigated in adsorbing copper ion (II), up to 19.9 mg/g, under different pH values from 2 to 6. Shi et al. [9] combined the merits of both sulfonic acid and thio-loaded silica to show the good purifying capacity in the multicomponent wastewater, containing different organic dyes and metal ions. Other works have prepared organo-sulfonic groups-modified mesoporous silica as catalysts and adsorbents [10–14].

Two major approaches in modifying the filler surface included 'grafting to" and "grafting from" methods [15]. Zdyrko et al. [16] pointed out the merit of the "grafting to" method over the "grafting from" method in their recent review for several polymers, including polystyrene [17], sulfonated polymers [18], etc. The "grafting from" method often involves the polymerization initiated from the molecular moiety pre-grafted on the filler surface [19, 20], thus it is sometimes difficult in controlling the grafted molecular weight on the filler surface. Whereas, the pre-synthesized polymer with well-defined molecular weight onto the filler surface could be easily attained via the "graft to" reaction. It is our attempt to prepare functionalized silica through this "graft to" approach. In this work, two types of silanes, including epoxy and aminosilanes, were grafted onto PSSA_MA first, followed by the grafting reaction to the silica surface. The possible reaction mechanism for two different silanes is proposed. The epoxysilane was designed to react with maleic acid groups on PSSA_MA. On the other hand, the aminosilane most interacted with sulfonic acid groups on PSSA_MA. This selective reaction endowed functionalized silica with tailored functionality for the specific application, such as harvesting certain metal ions. Represented ions, including Fe (III) and Cu(II), were adsorbed for these modified silica. To the authors' best knowledge, there is no literature available to prepare PSSA_MA grafted nanosilica via two different types of silanes. Without the use of the coupling agents, the grafting degree of PSSA_MA was very limited. This work aims to unveil this selective surface modification on the silica surface. Hopefully, this could signify the importance of coupling agent for better understanding the effect of surface modification role in organic/inorganic hybrid systems.

Experimental

Materials

Polystyrene sulfonic acid-co-maleic acid (PSSA_MA, sulfonic acid: maleic acid = 3:1) with the weight average molecular weight of 20,000 g/mole and a density of 0.8 g/cm^3 were obtained from Sigma. To the authors' best knowledge, the selected copolymer is a random copolymer according to the literature works, which have used this copolymer to prepare fuel cell membranes [21–24]. A detail structure characterization was also addressed elsewhere in the literature [25]. 1-ethyl-3-(3-dimethylaminopropyl)-carbodiimide (EDC) as the activating agent with the molecular weight of 155 g/mole was received from Sigma as well. Tetraethoxysilane (TEOS), 3-aminopropyltriethoxysilane (APTES), and 3-glycidoxypropyltrimethoxysilane (GPTMS) were purchased from Acros. Ammonium hydroxide was procured from Showa. Ethanol and sodium hydroxide were purchased from Echo.

Sample preparations

The main purpose of this study is to fabricate organically modified silica hybrid adsorbents. Silica was modified using polystyrene sulfonic acid-co-maleic acid (PSSA_MA) pretreated with two different coupling agents, including 3-aminopropyltriethoxysilane (APTES) and 3-glycidoxypropyltrimethoxysilane (GPTMS). The detail procedures were listed below.

Nanosilica colloidal particles were prepared according to the Stöber method [26] by controlling the various amounts of reactants (TEOS) and catalyst (ammonium hydroxide). First, deionized water (135 mL), ethanol (469 mL), and ammonium hydroxide (14.6 mL) were thoroughly mixed to form a homogeneous solution at room temperature, followed by the addition of tetraethoxysilane (TEOS) of 31.0 mL with a vigorous stirring for 1 h. Additional ethanol of half volume of previous homogenized solution was added to adjust pH value till 11. The silica solution was centrifuged at 5500 rpm, thoroughly washed with deionized water and ethanol, and then freeze-dried at −30 °C for 28 h to obtain silica particles. A further modification using two different silanes and PSSA_MA was described below.

PSSA_MA-APTES-Silica

First, 1 g of PSSA_MA was added to the mixture of 80 mL of deionized water and 20 mL of ethanol in a 250 mL glass beaker to form a homogeneous solution. Secondly, 0.1 g of 1-ethyl-3-(3-dimethylaminopropyl)-carbodiimide (EDC) to active the carbonyl group on PSSA_MA was added to the above solution for the reaction with the following addition of 1 mL of aminosilane at room temperature for 16 h. The solution was then centrifuged at 14000 rpm for 20 min at room temperature to separate the gel portion from self-condensation of aminosilane. Finally, the upper layer of homogeneous mixture was sampled and thoroughly stirred with 1 g of silica particles in a three-necked flask equipped with a mechanical

stirrer at 80 °C for 3 h of reaction. After the modified silica solution was cooled to room temperature, a rotary evaporator was employed to obtain the concentrate. The silica concentrate was centrifuged at 5500 rpm, thoroughly washed with deionized water and ethanol, and then freeze-dried at −30 °C for 28 h to obtain PSSA_MA-APTES-Silica particles.

PSSA_MA-GPTMS-Silica

First, 1 g of PSSA_MA was prepared as described in the previous section. Secondly, 1 mL of epoxysilane was added to homogenous solution for 24 h at the temperature of 50 °C. Then, PSSA_MA-GPTMS-Silica particles were prepared as described in the aminosilane grafting process earlier.

Measurements

Structure characterization

The modified silica was examined by Fourier transform infrared spectrometer (Perkin-Elmer, Connecticut, USA, Spectrum 100, FT-IR) at a resolution of 4 cm^{-1} for 16 scans from 4000 to 400 cm^{-1}.

Morphological characterization

Transmission electron microscopy (TEM) was employed to evaluate the morphology of silica with a Hitachi H-7100 using an acceleration voltage of 75 kV.

Thermal characterization

The amount of grafted silica and the thermal stability of the composites were determined by thermogravimetric analysis (Perkin-Elmer, Connecticut, USA, Pyris 1 TGA). The thermogravimetric analysis was carried out in the temperature range from 30 to 100 °C with a holding time of 10 min at 100 °C to remove the adsorbed water first, followed by heating to 800 °C at a heating rate 20 °C/min in a nitrogen environment. The grafting ratio was calculated based on the literature [27] as below,

$$\text{Grafting ratio } (\%) = \left(W_g - W_s\right) \Big/ \left(W_m - W_s\right) \times 100\%$$

Where, W_g is the residual weight of grafted silica, W_s is the residual weight of the pristine silica, W_m is the residual weight of silane modifiers. The residual weight was based on the weight loss difference at the temperature between 800 and 100 °C.

Adsorption

The standard sample solution was prepared by diluting standard solution of Cu(II) and Fe(III), respectively. Solutions containing initial concentrations of metal ions at 25, 30, 50, 100, and 200 ppm were prepared. 0.15 g of the sorbent was added to each solution at room temperature. The adsorption experiment was carried out at pH = 5 for Cu (II) and pH = 2 for Fe (III) to avoid the ion precipitation at higher pH values for a contact time of 180 min. After the adsorption experiment, we measured the concentration of solution by atomic absorption spectrophotometer (Hitachi High-Technologies Corporation, Tokyo, Japan, Z-2000). The amounts of metal ions absorbed at equilibrium, q (mg/g), were calculated according to the following equation.

$$q = \frac{(C_o - C_e)}{W} V$$

Where, C_o and C_e (mg/g) were initial concentrations in the liquid phase and equilibrium concentrations of the metal ions, respectively. V represents the volume of the solution (cm^3), and W was the mass of sorbent (g).

Results and discussion

Structure characterization of modified silica

APTES system

To ensure a successful grafting reaction of PSSA_MA through aminosilane (APTES) onto silica, FTIR was employed to determine the characteristic functional groups. Major regions of the FTIR spectra of modified silica with or without PSSA_MA through aminosilane are depicted in Fig. 1 for comparison. The stretching peak assignments of Si-OH bonds at 960 cm^{-1} and Si-O-Si bonds at 1103, 800, and 470 cm^{-1} were the characteristic bands of control silica [28]. The characteristic functional groups of PSSA_MA included the C-H bending (1410 cm^{-1}), C-H stretching (2800–3000 cm^{-1}), C = C (1575 cm^{-1}), S-O stretching in SO_3H (1126 cm^{-1}), antisymmetric vibration in SO_3^- (1036 cm^{-1}), in-plane bonding vibration of phenyl ring (1005 cm^{-1}), and aromatic signal at 677 cm^{-1} [21, 29–31]. After the reaction of aminosilane with PSSA_MA, the characteristic absorption regions of PSSA_MA-APTES on C-H groups (2928 cm^{-1}), and Si-OH (950 cm^{-1}) were observed as indicated in the literature [32]. Basically, the results confirmed the effective reaction of aminosilane with PSSA_MA. After the incorporation of silica to react with PSSA_MA-APTES further, the weak absorption of C-H group (2931 cm^{-1}) was observed. Thus, the effective

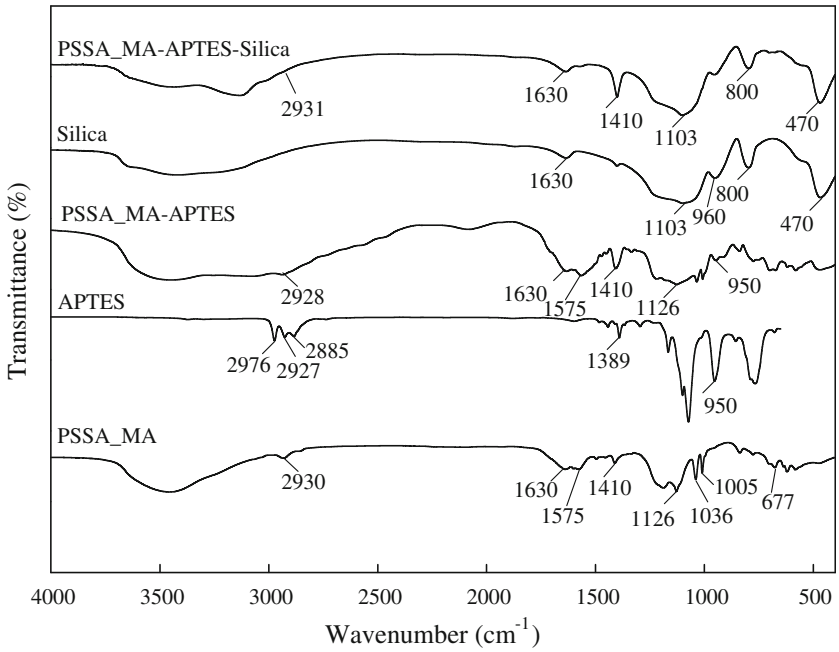

Fig. 1 FT-IR spectra of silica and modified silica (APTES system)

grafting of PSSA_MA onto silica through APTES was justified.

To further get more understanding on the potential reaction site of PSSA_MA with APTES, a control sample of polyacrylic acid (PAA) to simulate the carboxyl groups derived from maleic acid groups on PSSA_MA was employed to check if the amino groups on APTES could react with the carboxyl groups on PAA during the reaction process. Figure 2 shows the major regions of the FTIR spectra of PAA-APTES-Silica and pristine silica. Two additional absorption peaks at 1561 and 1450 cm^{-1} associating with the stretching absorption peaks of COO^- and C-H were observed for PAA-APTES-Silica [33]. This suggested that aminosilane was capable to react with PAA during the course of reaction, which further implied that aminosilane could also react with PSSA_MA through the maleic acid groups.

To further investigate the effect of EDC on the grafting site of PSSA_MA with aminosilane, Fig. 3 shows the grafting

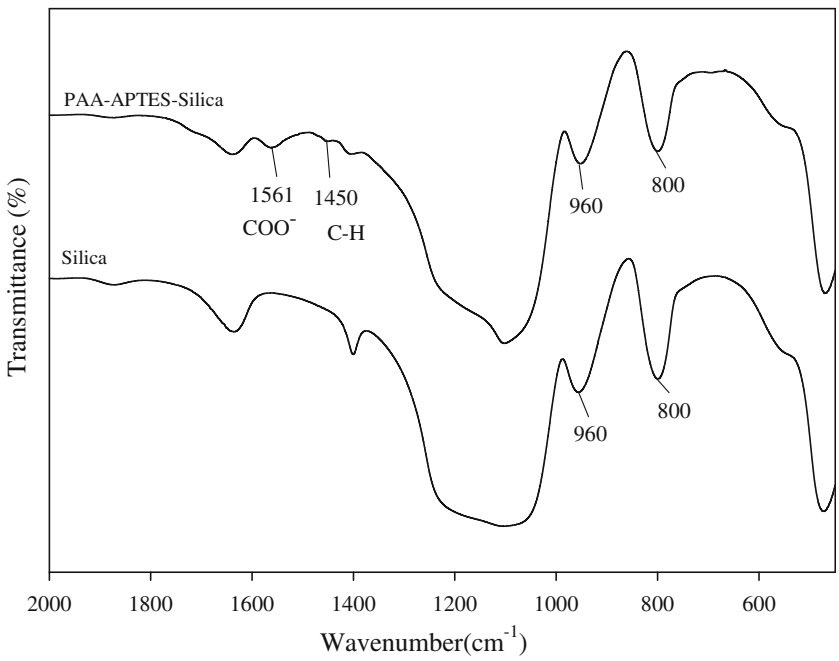

Fig. 2 FTIR spectra of PAA grafted silica

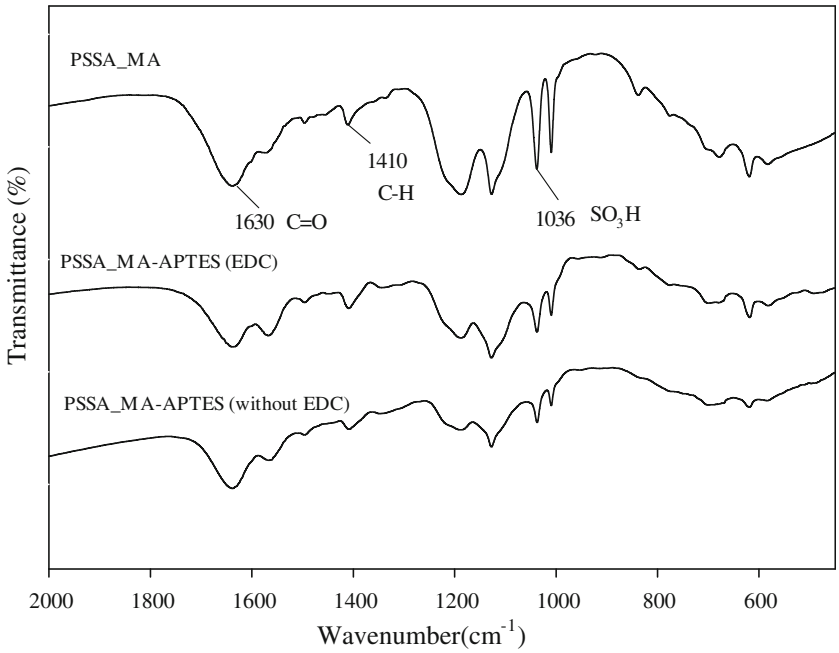

Fig. 3 FTIR spectra of PSSA_MA, PSSA_MA-APTES (EDC), and PSSA_MA-APTES (without EDC)

comparison with or without EDC. By evaluating the relative change in the peak area ratio of C = O and SO_3H with respect to that of C-H according to the literature [34, 35], the preferential reaction site between aminosilane and PSSA_MA could be elucidated. Without the activating agent, the peak area ratio of SO_3 with respect to C-H groups on PSSA_MA significantly changed from 2.0 to 1.1, but only a minor change for C = O from 5.6 to 4.7. This indicated that aminosilane preferentially interacted with sulfonic groups through ionic interaction. With the addition of EDC, the peak area ratio of SO_3 on PSSA_MA still reduced from 2.0 to 1.0, but a significant change for C = O from 5.6 to 1.3. The result suggested that aminosilane not only interacted with sulfonic groups but also the activated maleic acid groups via EDC activation.

GPTMS system

FTIR was also used to ensure a successful grafting reaction of epoxysilane (GPTMS) onto silica. Major regions of the FTIR spectra of modified silica with or without PSSA_MA are

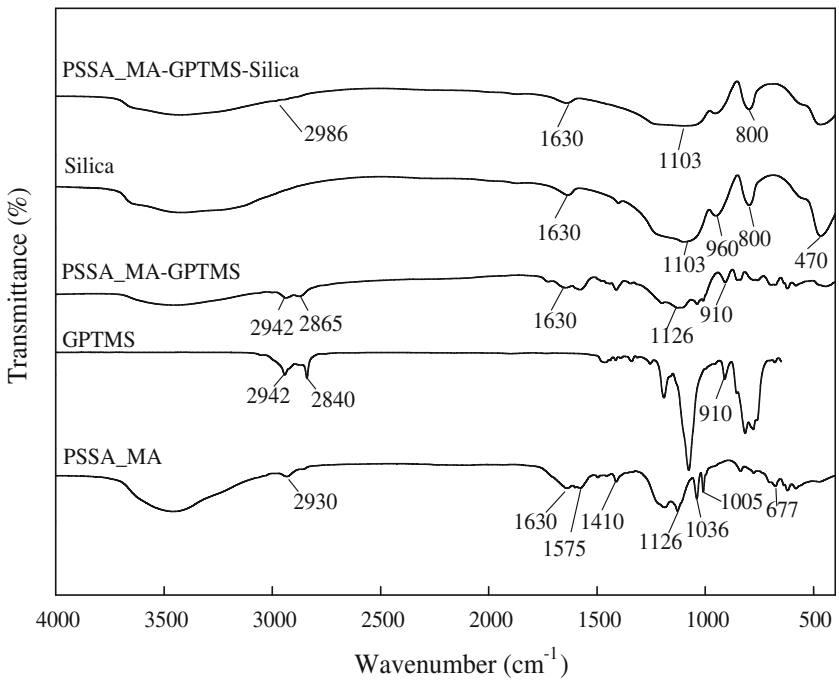

Fig. 4 FTIR spectra of silica and modified silica (GPTMS system)

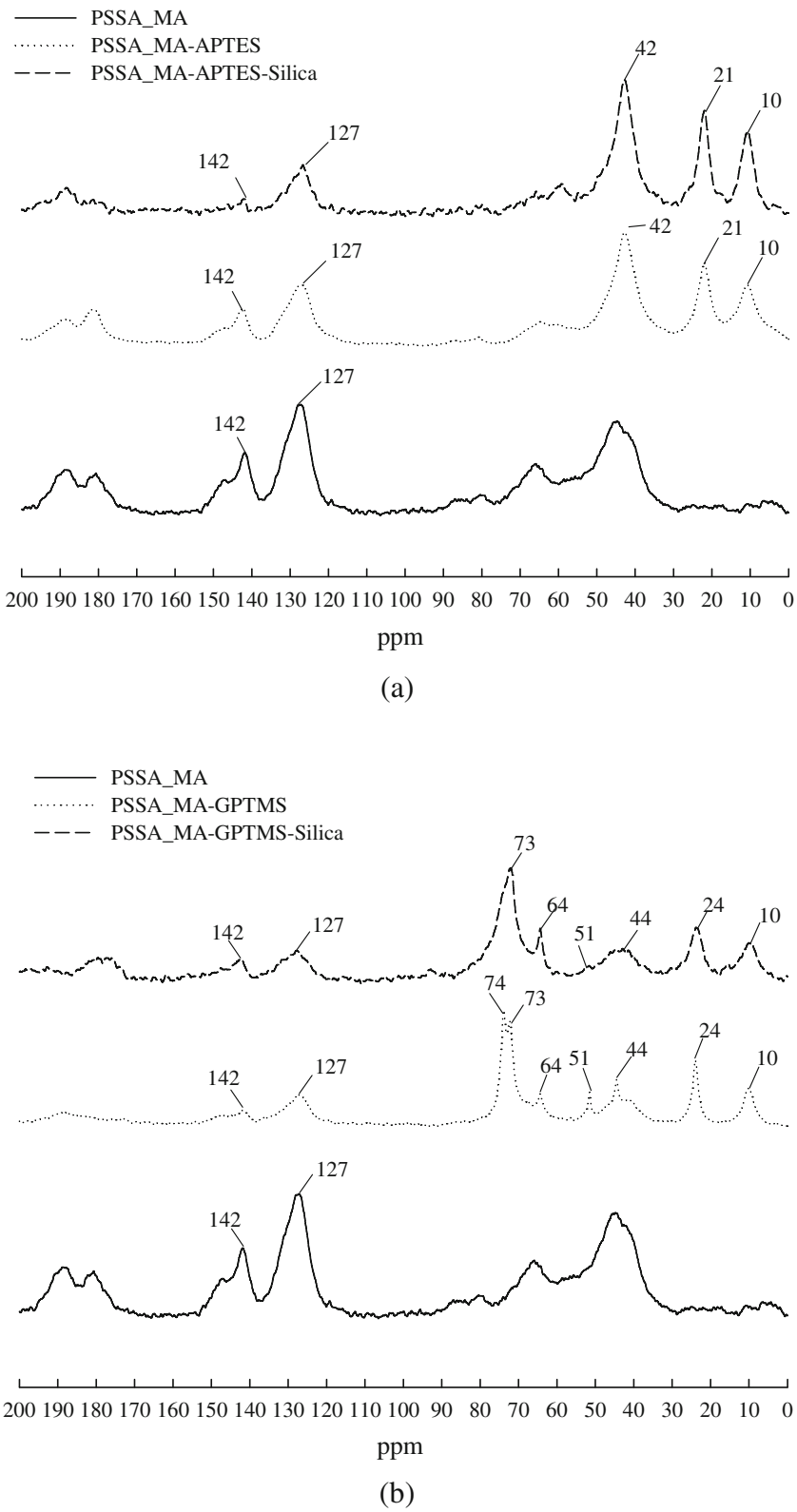

Fig. 5 Solid-state ^{13}C-NMR spectra of the PSSA_MA in the (**a**) APTES system (**b**) GPTMS system

depicted in Fig. 4 for comparison. The peak assignments of silica and PSSA_MA were as described earlier. After the epoxysilane grafted with PSSA_MA, the characteristic absorption regions of PSSA_MA-GPTMS on C-H groups (2942 and 2865 cm^{-1}), and epoxy peak (910 cm^{-1}) were observed as indicated in the literature [36]. Basically, the results confirmed the effective reaction of epoxysilane. After silica reacted with PSSA_MA-GPTMS further, the weak absorption

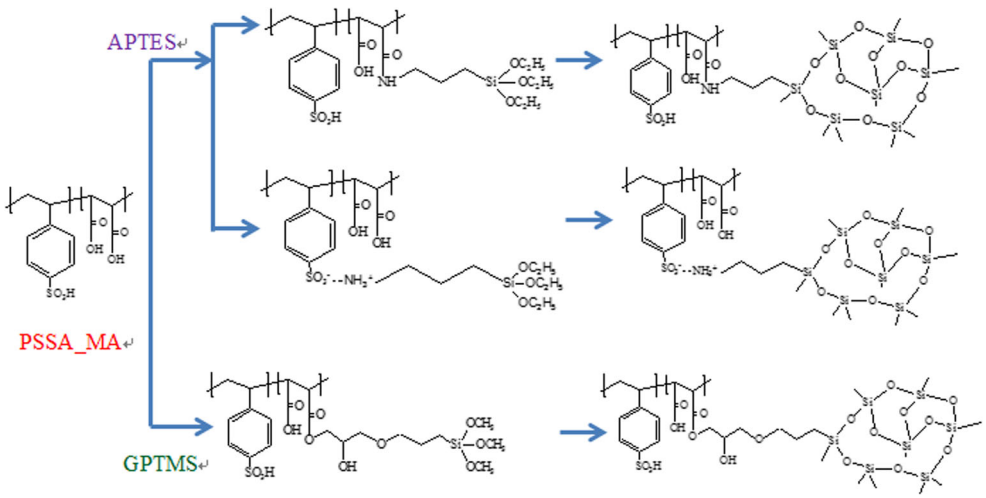

Fig. 6 Reaction mechanism of surface modified silica

of C-H group (2986 cm^{-1}) was observed. The C–H groups covered the wave numbers from 3000 to 2840 cm^{-1}, including asymmetrical and symmetrical stretches from -CH_3 and -CH_2. Although it was slightly difficult to identify the exact peak assignments of the weak band, yet it was still informative to provide the basic difference in the functional groups on the silica surface after the silane modification. Thus, the effective grafting of PSSA_MA onto silica through GPTMS was justified.

To further get the detail reaction route of PSSA_MA with GPTMS, a control sample of PSSA without the maleic acid groups on its main chain was employed to check if the epoxy groups could react with the sulfonic acid groups on PSSA during the reaction process. No clear difference between modified silica and pristine silica was observed in the major regions of the FTIR spectra of PSSA-GPTMS-Silica and pristine silica (omitted for brevity), indicating the lack of the reaction between epoxy groups and sulfonic acid groups. This suggested that epoxysilane tended to react with the PSSA_MA through the maleic acid groups, instead of sulfonic acid groups.

Reaction schemes

To further understand the detail structures of modified silica, ^{13}C NMR to reveal the information of carbon environment was conducted as shown in Fig. 5a and b, respectively. For ^{13}C analysis, the modified silica displayed strong resonance peaks assigned to chemical shifts at 10, 21, and 42 ppm,

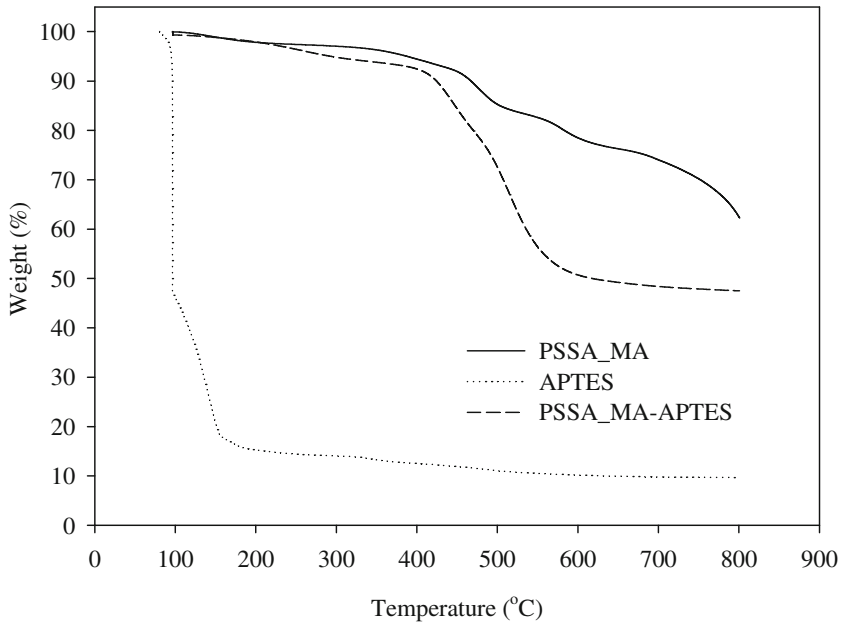

Fig. 7 TGA curves of PSSA_MA and APTES

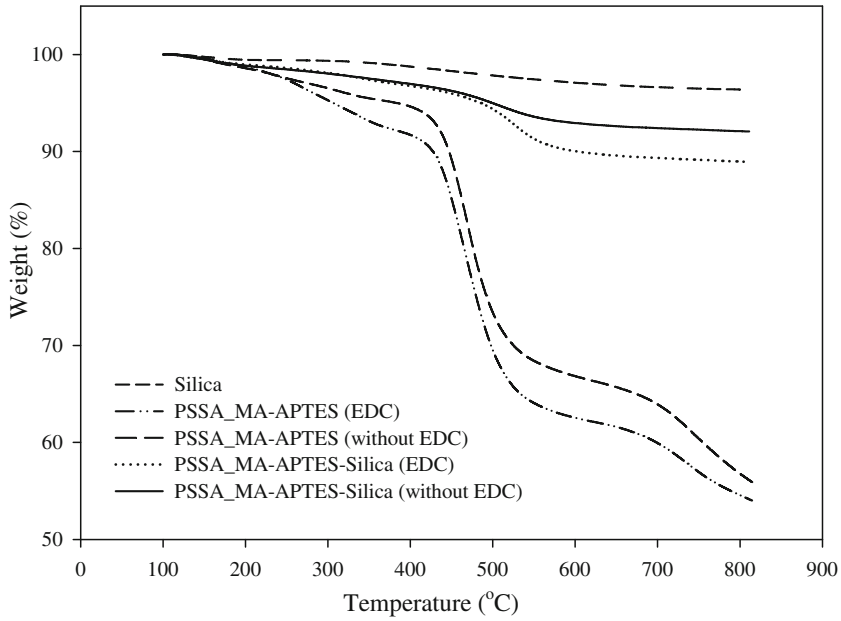

Fig. 8 TGA curves of modified silica in APTES systems (scaled to 100 °C)

respectively, to confirm the existence of aminosilane as shown in Fig. 5a [37, 38]. In the GPTMS system, the modified silica displayed strong resonance peaks assigned to chemical shifts at 10, 24, 44, 51, 64, and 73 ppm, respectively, to confirm the existence of epoxysilane as shown in Fig. 5b [39]. The overall reaction schemes for PSSA_MA modified silica are shown in Fig. 6. The result indicated that aminosilane not only interacted with sulfonic acid groups but also the activated maleic acid groups via EDC, on the other hand epoxysilane tended to react with the PSSA_MA through the maleic acid groups, instead of sulfonic acid groups.

Thermal characterization of modified silica

To investigate the effect of hybrids on the thermal resistance, thermogravimetric analysis was employed to evaluate the thermal stability of organic PSSA_MA first. According to Fig. 7, four main degradation stages were observed. The onset of weight loss of material was all shifted to 100 °C to consider the loss of water in the samples. Also, APTES showed relatively low thermal stability due to small organic molecule nature. The degradation temperatures increased for inorganic–organic hybrid materials, as shown in Fig. 8, since silica improved the thermal stability of PSSA_MA as generally seen in the inorganic particles-reinforced nanocomposite systems.

TGA was also employed to evaluate the grafting degree of PSSA_MA via APTES and GPTMS on the silica surfaces [40]. Figure 8 shows the thermal scans of silica nanoparticles modified with PSSA_MA via APTES with or without EDC. Table 1 shows the corresponding results of grafting ratio. Basically, the grafting ratio of PSSA_MA increased with the addition of EDC. Without EDC, the aminosilane with positive charge would mainly react with sulfonic acid groups with negative charge through the ionic interaction. This ionic interaction was perceived in the literature as well [41]. With the addition of EDC, maleic acid groups were successfully

Table 1 Grafting ratio of silica with different modifications

Sample code	100–800 °C Wt %	Grafting ratio %
PSSA_MA-GPTMS	43.8	–
PSSA_MA-GPTMS-Silica	9.4	14.4 %
PSSA_MA-APTES (EDC)	44.7	–
PSSA_MA-APTES (without EDC)	43.2	–
PSSA_MA-APTES-Silica (EDC)	11.0	18.0 %
PSSA_MA-APTES-Silica (without EDC)	7.9	10.9 %
Silica	3.6	–
PSSA_MA	46.2	–
PSSA_MA-Silica	4.9	3.0 %

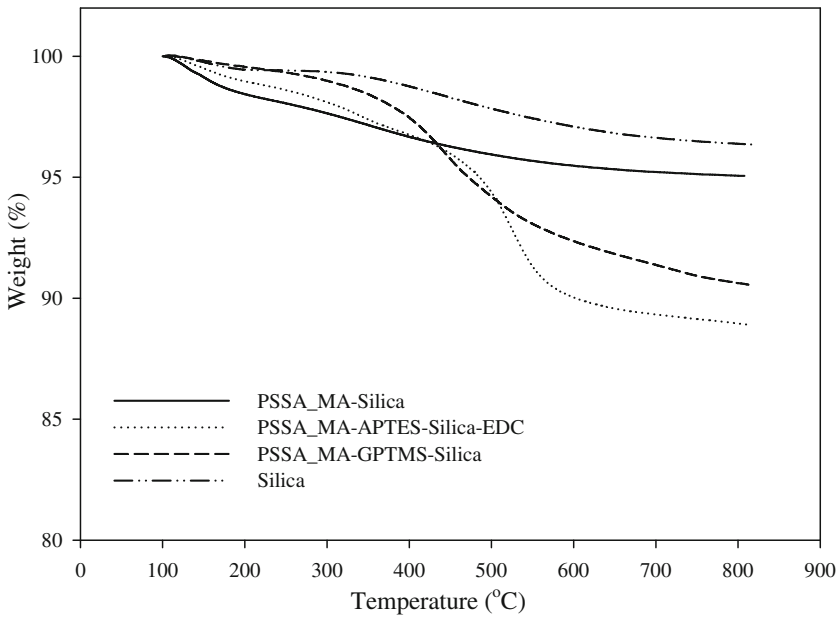

Fig. 9 TGA curves of silica, PSSA_MA-Silica, PSSA_MA-APTES-Silica (EDC) and PSSA_MA-GPTMS-Silica

activated to react amino groups on APTES [42–44], besides that partial ionic interaction. The grafting ratio of PSSA_MA via APTES with EDC thus reached 18.0 %. The EDC was reported to first react with carboxylic acid to form o-acrylisourea derivative, followed by the reaction with amine groups to form amide bond with the isourea derivative as the byproduct [43]. The detail coupling mechanisms addressed in two additional references are included [43, 44]. Thus, the function of EDC mainly acted as the activating agent to favor the coupling reaction for amidation between maleic acid groups on PSSA_MA and amine functional groups on APTES.

In order to react with PSSA_MA without the functionality of sulfonic acid groups, GPTMS was selected as another coupling agent to graft PSSA_MA onto the silica surface through the reaction of epoxy groups on GPTMS and maleic acid groups on PSSA_MA. The results of TGA curves are shown in Fig. 9 and Table 1. The grafting ratio reached 14.4 %, which was slightly lower than that of APTES case. Interestingly, if one compared the reactivity of GPTMS and APTES with MA on PSSA_MA, the effective grafting efficiency of GPTMS with MA was essentially higher than that of APTES in this study, because the factor of the molar ratio of SSA to MA in PSSA_MA was about 3 times and APTES tended to react with

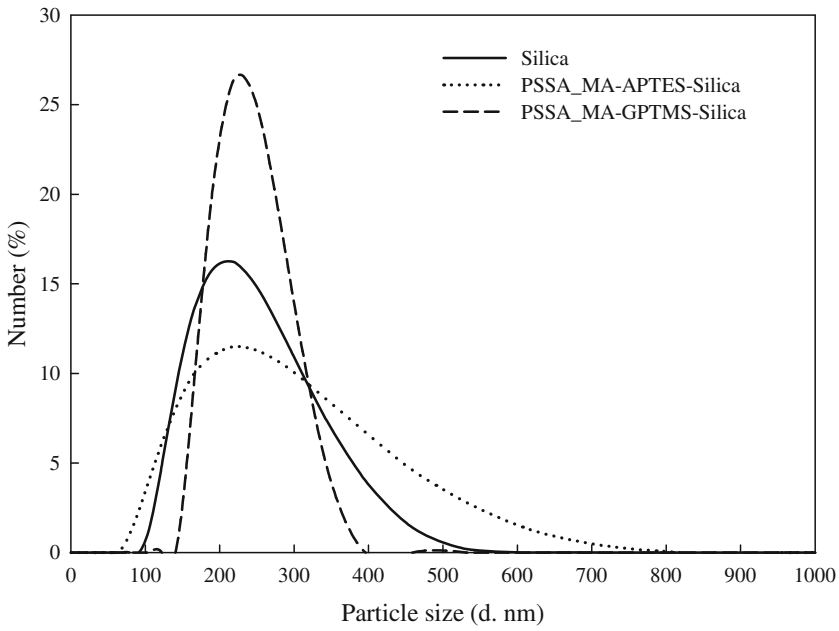

Fig. 10 Particles size distribution of silica and modified silica

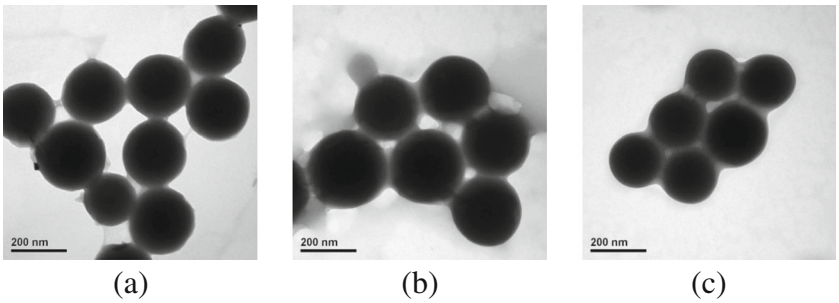

Fig. 11 TEM micrographs of (**a**) silica, (**b**) PSSA_MA-APTES-Silica, and (**c**) PSSA_MA-GPTMS-Silica (×50 kx)

SSA on PSSA_MA as well. Note that a control experiment on neat silica modified with PSSA_MA without pre-grafted APTES or GPTMS only showed 3 % grafted PSSA_MA, as seen in Table 1. It was suggested that coupling agents were essential to achieve a measurable amount of grafted PSSA_MA onto the silica surface.

Particle size characterization

Figure 10 shows no significant increase in the particle size after modification, except some large particles modified with APTES. In general, the particle size distribution was quite uniform. However, The APTES-modified system appeared to have a wider particle size distribution, which might be attributed to higher grafting amounts of PSSA_MA onto silica to increase their aggregation behaviors by increasing specific interaction, such as hydrogen bonding. Figure 11 shows the images of transmission electron microscopy to confirm the results of Zetaziser. The images showed that the average particle size of silica was around 200 nm. The results agreed well with those of the Zetasizer analysis.

Adsorption

As the addition of EDC increased the grafting ratio, so only the modified system containing EDC was selected for evaluation. Figure 12 shows the adsorption capacity of Fe (III) ion. Silica was known to have a good adsorption capacity of Fe (III) due to its hydroxyl functional groups [45]. Thus, the negative contribution from modified silica was observed due to the loss of hydroxyl groups through the silane reaction on the silica surface. As the grafting degree of PSSA_MA-APTES-Silica (EDC) was slightly higher than that of PSSA_MA-GPTMS-Silica, it was thought that PSSA_MA-GPTMS-Silica should render a higher adsorption capacity due to more residual OH groups on the silica surface. However, the opposite results were found, which indicated that some unreacted hydroxyl groups on maleic acid in PSSA_MA-APTES-Silica (EDC) was beneficial to compensate the loss of residual OH groups on the silica surface. As for the PSSA_MA-GPTMS-Silica case, epoxysilane only reacted with maleic acid, which resulted in the lower amount of hydroxyl groups on PSSA_MA. Regarding the effect of initial ion concentrations, the adsorption capacity increased in a

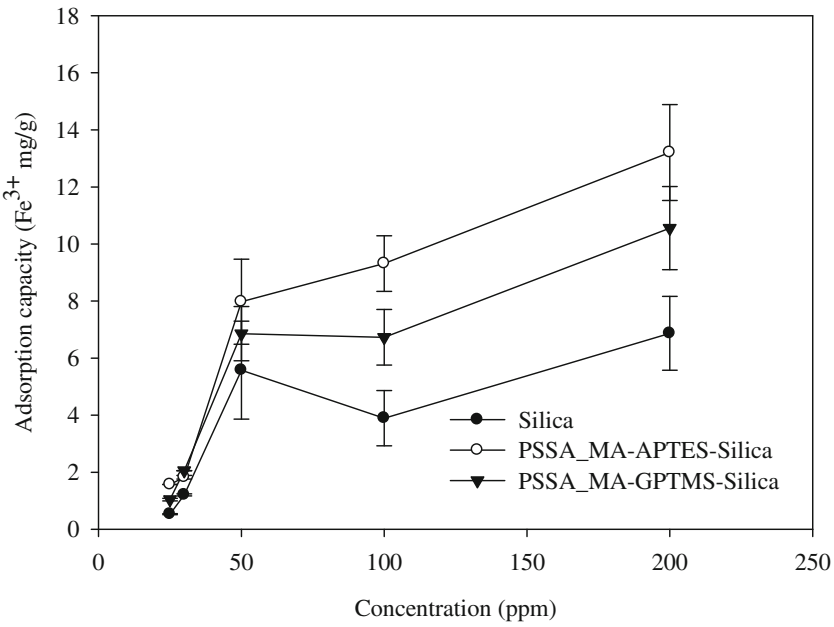

Fig. 12 Effect of the initial concentration on the adsorption of Fe (III) onto silica and modified silica

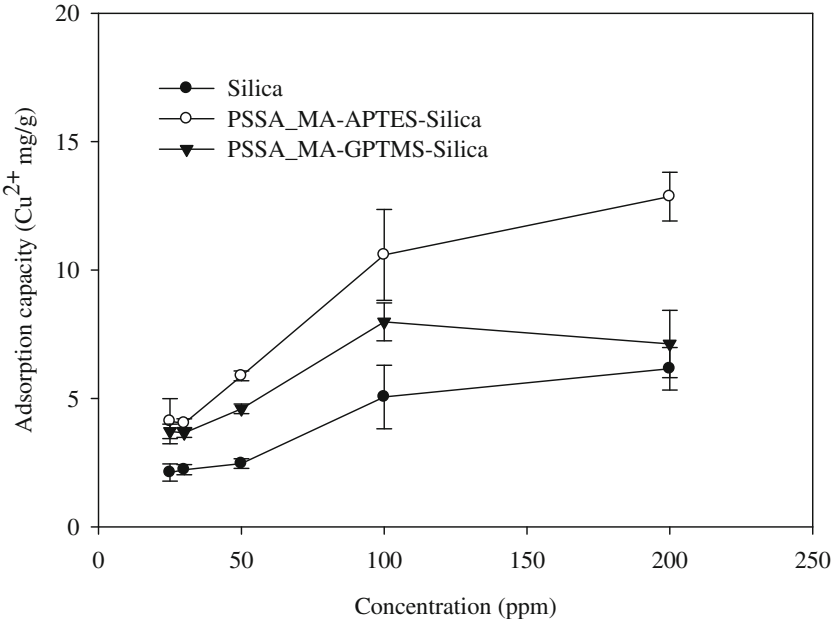

Fig. 13 Effect of the initial concentration on the adsorption of Cu (II) onto silica and modified silica

measurable degree at high concentrations. Strictly speaking, the difference at low initial ion concentrations was quite limited. In general, APTES-modified cases conferred the highest ion adsorption capacity.

By grafting PSSA_MA with sulfonic acid groups onto silica, the adsorption capacity was expected to increase for certain ion adsorption. The results on the adsorption of Cu (II) ion are shown in Fig. 13. Modified silica, either PSSA_MA-APTES-Silica (EDC) or PSSA_MA-GPTMS-Silica, possessed the higher adsorption capacity of copper than unmodified silica. The adsorption capacity tended to be increased with increasing initial concentrations and leveled off at higher concentrations. The maximum adsorption capacity of silica was 6.2 ± 0.8 mg/g at 200 ppm of initial concentration, and the values were about 12.9 ± 1.0 and 7.1 ± 1.3 mg/g for PSSA_MA-APTES-Silica (EDC) and PSSA_MA-GPTMS-Silica cases, respectively. Apparently, the APTES-modified samples showed the highest improvement in the Cu(II) ion adsorption capacity in all investigated cases.

Conclusions

Two types of functional silanes, including 3-glycidoxypropyltrimethoxysilane and 3-aminopropyltriethoxysilane, were grafted onto polystyrene sulfonic acid-co-maleic acid first, followed by the grafting reaction to the silica surface. The functional groups and grafting degrees on silica could be tailored via the silane modification of PSSA_MA. The grafting ratio of PSSA_MA via APTES with 1-ethyl-3-(3- dimethylaminopropyl)-carbodiimide activation reached 18.0 %. As for GPTMS case, the grafting ratio reached 14.4 %. The epoxysilane was found to react with maleic acid groups on PSSA_MA only. On the other hand, aminosilane not only interacted with sulfonic acid groups but also the activated maleic acid groups via EDC. However, without the use of the coupling agents, the grafting degree of PSSA_MA was very limited. Average particle size of silica was around 200 nm with or without organic modification from the transmission electron microscopy (TEM) and Zetasizer analysis. This modification helps to improve the adsorption of metal ions in a great degree.

Acknowledgments The partial grants-in-aid from R.O.C. government under the contract number of NSC 100-2221-E-197-029– and Stone and Resource Industry R&D Center are greatly acknowledged. We are also grateful to Dr. Ming-Hong Ku for helpful discussion.

References

1. Brinker CJ, Sherer GW (1990) Sol–gel science: the physics and chemistry of sol–gel processing. Academic Press, San Diego
2. Philipp G, Schmidt HJ (1984) New materials for contact lenses prepared from Si- and Ti-alkoxides by the sol–gel process. J Non-Cryst Solids 63:283–292
3. Wilkes GL, Orler B, Huang H (1985) Ceramers: Hybrid materials incorporating polymeric/oligomeric species into inorganic glasses utilizing a sol–gel approach. Polym Prepr 26:300–301
4. Pan B, Pan B, Zhang W, Lv L, Zhang Q, Zheng S (2009) Development of polymeric and polymer-based hybrid adsorbents for pollutants removal from waters. Chem Eng J 151:19–29
5. Pan BC, Zhang QR, Zhang WM, Pan BJ, Du W, Lv L, Zhang QJ, Xu ZW, Zhang QX (2007) Highly effective removal of heavy metals by polymer-based zirconium phosphate: a case study of lead ion. J Colloid Interface Sci 310:99–105
6. Qu Q, Gu Q, Gu Z, Shen Y, Wang C, Hu X (2012) Efficient removal of heavy metal from aqueous solution by sulfonic acid functionalized nonporous silica microspheres. Colloids Surf A Physicochem Eng Asp 415:41–46

7. Shevchenko N, Zaitsev V, Walcarius A (2008) Bifunctionalized mesoporous silicas for Cr(VI) reduction and concomitant Cr(III) immobilization. Environ Sci Technol 42:6922–6928
8. Wang H, Kang J, Liu H, Qu J (2009) Preparation of organically functionalized silica gel as adsorbent for copper ion adsorption. J Environ Sci 21:1473–1479
9. Shi W, Tao S, Yu Y, Wang Y, Ma W (2011) High performance adsorbents based on hierarchically porous silica for purifying multicomponent wastewater. J Mater Chem 21:15567–15574
10. Hozhabr Araghi S, Entezari MH (2015) Amino-functionalized silica magnetite nanoparticles for the simultaneous removal of pollutants from aqueous solution. Appl Surf Sci 333:68–77
11. Chen H, Wang W, Wei X, Ding J, Yang J (2015) Experimental and numerical study on water sorption over modified mesoporous silica. Adsorption 21:67–75
12. Sasidharan M, Bhaumik A (2013) Novel and mild synthetic strategy for the sulfonic acid functionalization in periodic mesoporous ethenylene-silica. ACS Appl Mater Interfaces 5:2618–2625
13. Gehring J, Schleheck D, Luka M, Polarz S (2014) Aerosol-synthesis of mesoporous organosilica nanoparticles with highly reactive, superacidic surfaces comprising sulfonic acid entities. Adv Funct Mater 24:1140–1150
14. Azmiyawati C, Nuryono N (2014) Synthesis of disulfonato-silica hybrid from rice husk ash. J Med Bioeng 3:301–305
15. Zou H, Wu S, Shen J (2008) Polymer/silica nanocomposites: preparation, characterization, properties, and applications. Chem Rev 108:3893–3957
16. Zdyrko B, Luzinov I (2011) Polymer brushes by the "grafting to" method. Macromol Rapid Commun 32:859–869
17. Corbierre MK, Cameron NS, Sutton M, Laaziri K, Lennox RB (2005) Gold nanoparticle/polymer Nanocomposites: dispersion of nanoparticles as a gunction of capping agent molecular weight and grafting density. Langmuir 21:6063–6072
18. Mahdavi H, Ahmadian-Alam L (2015) Sulfonic acid functionalization of 2-aminoterephthalate metal−organic framework and silica nanoparticles by surface initiated radical polymerization: as proton-conducting solid electrolytes. J Polym Res 22: 67–78
19. Zou T, Zhou Z, Dai J, Gao L, Wei X, Li C, Guan W, Yan Y (2014) Preparation of silica-based surface-imprinted core-shell nanoadsorbents for the selective recognition of sulfamethazine via reverse atom transfer radical precipitation polymerization. J Polym Res 21:520–531
20. Gao B, Shi N, Shi X (2013) Preparation of grafted particles PGMA/SiO_2 with a new surface-initiating system of mercapto group/BPO and their functionalization transformation. J Polym Res 20:260–269
21. Kim DS, Guiver MD, Nam SY, Yun TI, Seo MY, Kim SJ, Hwang HS, Rhim JW (2006) Preparation of ion exchange membranes for fuel cell based on crosslinked poly(vinyl alcohol) with poly(styrene sulfonic acid-co-maleic acid). J Membr Sci 281:156–162
22. Seo JA, Koh JH, Roh DK, Kim JH (2009) Preparation and characterization of crosslinked proton conducting membranes based on chitosan and PSSA-MA copolymer. Solid State Ionics 180:998–1002
23. Ye YS, Rick J, Hwang BJ (2012) Water soluble polymers as proton exchange membranes for fuel cells. Polymers 4:913–963
24. Boonpoo-nga R, Sriring M, Nasomjai P, Martwiset S (2014) Electrospun fibres from polyvinyl alcohol, poly(styrenesulphonic acid-co-maleic acid), and imidazole for proton exchange membranes. Sci Asia 40:232–237
25. Stewart EA (2006) Applications of Mass Spectrometry to Synthetic Copolymers Master's Thesis, University of Tennessee.
26. Kim JW, Kim LU, Kim CK (2007) Size control of silica nanoparticles and their surface treatment for fabrication of dental nanocomposites. Biomacromolecule 8:215–222
27. Guo Y, Wang M, Zhang H, Liu G, Zhang L, Qu X (2008) The surface modification of nanosilica, preparation of nanosilica/acrylic core-shell composite latex, and its application in toughening PVC matrix. J Appl Polymer Sci 107:2671–2680
28. Ray S, Bhowmick AK (2002) Novel electron beam-modified surface-coated silica fillers: physical and chemical characteristics. J Appl Polym Sci 83:2255–2268
29. Socrates G (2001) Infrared and Raman Characteristic Group Frequencies: Tables and Charts. 3rd Edition, Wiley
30. Saxena A, Tripathi BP, Shahi VK (2007) Sulfonated poly(styrene-*co*-maleic anhydride)−poly(ethylene glycol)−silica nanocomposite polyelectrolyte membranes for fuel cell applications. J Phys Chem B 111:12454–12461
31. Xu L, Li X, Zhai M, Huang L, Peng J, Li J, Wei G (2007) Ion-specific swelling of poly(styrene sulfonic acid) hydrogel. J Phys Chem B 111:3391–3397
32. Viart N, Nizansky D, Rehspringer JL (1997) Structural evolution of a formamide modified sol—spectroscopic study. J Sol-Gel Sci Technol 8:183–187
33. Hu Y, Jiang X, Ding Y, Ge H, Yuan Y, Yang C (2002) Synthesis and characterization of chitosan–poly(acrylic acid) nanoparticles. Biomaterials 23:3193–3201
34. Ye YS, Chen WY, Huang YJ, Cheng MY, Yen YC, Cheng CC, Chang FC (2010) Preparation and characterization of high-durability zwitterionic crosslinked proton exchange membrane. J Membr Sci 362:29–37
35. Tanaka S, Chao Y, Araki S, Miyake Y (2010) Pervaporation characteristics of pore-filling PDMS/PMHS membranes for recovery of ethyl acetate from aqueous solution. J Membr Sci 348:383–388
36. Isin D, Kayaman-Apohan N, Gungor A (2009) Preparation and characterization of UV-curable epoxy/silica nanocomposite coatings. Prog Org Coat 65:477–483
37. Chang K-C, Lin C-Y, Lin H-F, Chiou S-C, Huang W-C, Yeh J-M, Yang J-C (2008) Thermally and mechanically enhanced epoxy resin-silica hybrid materials containing primary amine-modified silica nanoparticles. J Appl Polym Sci 108:1629–1635
38. Ek S, Iiskol EI, Niinist L, Vaittinen J, Pakkanen TT, Root A (2004) A ^{29}Si and ^{13}C CP/MAS NMR study on the surface species of gas-phase-deposited γ-aminopropylalkoxysilanes on heat-treated silica. J Phys Chem B 108:11454–11463
39. Lee DK, Won J, Hwang SS (2009) Effect of the matrix on proton conductivity in electrolyte membranes containing deoxyribonucleic acids. J Membr Sci 328:211–218
40. Heikkinen JJ, Heiskanen JP, Hormi OEO (2006) Grafting of functionalized silica particles with poly(acrylic acid). Poly Adv Technol 17:426–429
41. Donia AM, Atia AA, Al-Amrani WA, El-Nahas AM (2009) Effect of structural properties of acid dyes on their adsorption behaviour from aqueous solutions by amine modified silica. J Hazard Mater 30:1544–1550
42. Ye P, Xu Z-K, Che A-F, Wu J, Seta P (2005) Chitosan-tethered poly(acrylonitrile-co-maleic acid) hollow fiber membrane for lipase immobilization. Biomaterials 26:6394–6403
43. Lin D-J, Lin D-T, Young T-H, Huang F-M, Chen C-C, Cheng L-P (2004) Immobilization of heparin on PVDF membranes with microporous structures. J Membr Sci 245:137–146
44. Lloyd DR, Burns CM (1979) Coupling of acrylic polymers and collagen by use of a water-soluble carbodiimide. II. Investigations of the coupling mechanisms. J Polym Sci: Polym Chem 17:3459–3472
45. Bernabe L, Rivas MJ, Eduardo DP (2002) Preparation and adsorption properties of the chelating resins containing carboxylic, sulfonic, and imidazole groups. J Appl Polym Sci 89:2852–2856